Article citation info:
CHENG Q, SUN B, ZHAO Y, GU P. A method to analyze the machining accuracy reliability sensitivity of machine tools based on Fast Markov Chain simulation. Eksploatacja i Niezawodnosc – Maintenance and Reliability 2016; 18 (4): 552–564, http://dx.doi.org/10.17531/ein.2016.4.10.

Qiang CHENG
Bingwei SUN
Yongsheng ZHAO
Peihua GU

A METHOD TO ANALYZE THE MACHINING ACCURACY RELIABILITY SENSITIVITY OF MACHINE TOOLS BASED ON FAST MARKOV CHAIN SIMULATION

PODEJŚCIE DO ANALIZY CZUŁOŚCI NIEZAWODNOŚCIOWEJ DOKŁADNOŚCI OBRABIAREK OPARTE NA SYMULACJI METODĄ SZYBKICH ŁAŃCUCHÓW MARKOWA

With the ever increasing demand of higher machining accuracies, the machining accuracy reliability has evolved into an indicator to evaluate the performance of a machine tool. Consequentially, methods for improving the machining accuracy reliability have become the focus of attention for both manufacturers and users. Generally, the intercoupling geometric errors are the main cause which may lead to a reduction of the machining accuracy of machine tools. In this paper, the machining accuracy reliability is defined as the ability of a machine tool to perform at its specified machining accuracy under the stated conditions for a given period of time, and a new approach for analyzing the machining accuracy reliability of machine tools based on fast Markov chain simulations is proposed. Using this method, seven different failure modes could be determined for a machine tool. An analysis of the machining accuracy reliability sensitivity was performed based on solving the integral of the failure probability of the machine tool, and the key geometric errors which most strongly affect the machining accuracy reliability were identified. Finally, in this study, a 4-axis machine tool was selected as an example to experimentally validate the effectiveness of the proposed method.

Keywords: *machining accuracy reliability, machine tool, Fast Markov Chain, reliability sensitivity analysis, integral of failure probability.*

Wraz z wciąż rosnącym zapotrzebowaniem na coraz to wyższą dokładność obróbki, niezawodność dokładności obróbki stała się wskaźnikiem pozwalającym na ocenę charakterystyk obrabiarek. W rezultacie, metody doskonalenia niezawodności dokładności obróbki znalazły się w centrum uwagi zarówno producentów jak i użytkowników tych maszyn. Na ogół, do zmniejszenia dokładności obróbki prowadzą nakładające się błędy geometryczne. W niniejszej pracy, niezawodność dokładności obróbki zdefiniowano jako zdolność obrabiarki do pracy z określoną dla niej dokładnością w zadanych warunkach przez dany okres czasu. Zaproponowano nowe podejście do analizy niezawodności dokładności obróbki oparte na symulacji metodą szybkich łańcuchów Markowa. Za pomocą tej metody, można ustalić siedem różnych przyczyn uszkodzeń obrabiarki. Analizę czułości niezawodnościowej dokładności obróbki przeprowadzono obliczając całkę prawdopodobieństwa uszkodzenia obrabiarki. Określono także kluczowe błędy geometryczne, które najsilniej wpływają na niezawodność dokładności obróbki. Wreszcie, efektywność proponowanej metody sprawdzono doświadczalnie na przykładzie obrabiarki czteroosiowej.

Słowa kluczowe*: niezawodność dokładności obróbki, obrabiarka, szybki łańcuch Markowa, analiza czułości niezawodnościowej, całka prawdopodobieństwa uszkodzenia.*

1. Introduction

Multi-axis CNC machine tools are typical mechatronic devices with high added value and a wide range of applications. Achieving a high machining accuracy is adamant to ensure a high quality and performance of the machined mechanical product and the machining accuracy is therefore an important consideration for any manufacturer [30]. Machining accuracy is influenced by machining errors belonging to several categories, e.g. kinematics errors, thermal errors, cutting force induced errors, servo errors and tool wear [3]. It is influenced by a variety of machining errors which can be divided into several categories, e.g., kinematics errors, thermal errors, errors induced by the cutting force, servo errors and tool wear [3]. Among these different error sources, the geometric error of the machine tool components and structures is one of the biggest sources of inaccuracy, accounting for about 40% of all errors. Therefore, methods for improving the machining accuracy of CNC machine tools have become a hot topic recently.

1.1. Volumetric error model

In order to improve the machining accuracy of CNC machine tools, the theoretical modeling of errors is crucial to maximize the performance of these machine tools [4]. Error modeling can provide a systematic and suitable way to establish the error model for a given CNC machine tool. In recent years, many studies have focused on modeling multi-axis machine tools to determine the resultant error of individual components in relation to the set-point deviation of the tool and the workpiece. Furthermore, the various methods for modeling the geometric errors from different perspectives have experienced a gradual development [7]. To describe the error of the cutter location and the tool orientation between the two kinematic chains, the error model is normally established using homogeneous transformation

matrices (HTM) [10, 18, 20], denavit-hartenberg (D-H) method [16], modified denavit-hartenberg (MD-H) method [19], or multi-body system (MBS) theory [31, 32]. Among these different approaches, MBS theory, first proposed by Houston, has evolved into the best method for the modeling of geometric errors of machine tools because it provides for a simple and convenient method to describe the topological structure of an MBS [21].

1.2. Reliability analysis

After the error model for a given machine tool has been established, the next step is to study the machine tool's machining accuracy reliability. Recently, several studies have been published which reported on the reliability of mechanical systems from different perspectives. For instance, Du *et al*. has summarized three useful ways to improve the reliability of a machine, including (1) changing the mean values of random variables, (2) changing the variances of random variables, and (3) a truncation of the distributions of random variables [9]. Tang proposed a new method based on graph theory and Boolean functions for assessing the reliability of mechanical systems [26]. Avontuur and van der Werff proposed a new method for analyzing the reliability of mechanical and hydraulic systems based on finite element equations, which describe the motion of and the equilibrium between internal and external loads for structures and mechanisms [1]. Lin investigated the reliability and failure of face-milling tools when cutting stainless steel and the effect of different cutting conditions (cutting speed, feed, cutting depth) on the tool life [22]. Chen et al. performed a reliability estimation for cutting tools based on a logistic regression model using vibration signals [5]. However, to the best of our knowledge, there have been no studies on the machining accuracy reliability of CNC machine tools. The machining accuracy reliability refers to the tool's ability to perform at its specified machining accuracy. In general, the volumetric error of a machine tool can be divided into the errors corresponding to the X-, Y-, and Z-directions, respectively. The machining errors in each direction are likely to exceed the required machining accuracy, thereby effectively rendering the machine inaccurate and unreliable, and thus unusable. Consequentially, the machining accuracy of a machine tool is related to many different failure modes.

1.3. Sensitivity analysis

However, many different geometric errors have to be taken into account when modeling a multi-axis machine tool. For example, there are 29 geometric errors for a 4-axis machine tool. These geometric errors are interacting, and how to determine their degree of influence on the machining accuracy reliability is currently a difficult problem of machine tool design [14, 40]. Performing a sensitivity analysis is one possibility to identify and quantify the relationships between input and output uncertainties [29]. A variety of sensitivity analysis methods have been published in literature. For instance, Ghosh *et al*. proposed a new approach for a stochastic sensitivity analysis based on first-order perturbation theory [12]. Chen *et al*. established a volumetric error model and performed a sensitivity analysis for a 5-axis ultra-precision machine tool [6]. Based on the results of the local sensitivity analysis, they were able to slightly reduce the key error components, which made it easier to control the accuracy of the machine tool [6]. Cheng *et al*. considered the stochastic characteristic of the geometric errors and employed Sobol's global sensitivity analysis method to identify the crucial geometric errors of a machine tool, which is helpful for improving the machining accuracy of multi-axis machine tools [7]. De-Lataliade *et al*. developed a method based on Monte Carlo simulations (MCS) for estimating the reliability sensitivity [8]. Xiao *et al*. considered both epistemic and aleatory uncertainties in their reliability sensitivity analysis and proposed a unified reliability sensitivity estimation method for both epistemic and aleatory uncertainties by integrating the principles of a p-box, interval arithmetic, FORM, MCS, and weighted regression [28]. Guo and Du proposed a sensitivity analysis method for a mix of random and interval variables and defined six sensitivity indices for evaluating the sensitivity of the average reliability and reliability bounds with respect to the averages and widths of the intervals [13]. A sensitivity analysis of the geometric errors allows to identify the most critical geometric errors and then to strictly control them, thereby significantly improving the machining accuracy of the machine tool [24, 27]

Improving the machining accuracy reliability of machine tools is an important goal for both manufacturers and users, and two tasks are usually involved to accomplish it: 1) to express and measure the machine accuracy reliability of the machine tool; 2) to identify the most critical geometric errors that most strongly affect the machining accuracy reliability of each failure mode. In this study, the sensitivity analysis was used to provide information for the reliability-based design based on solving the integral of the failure probability.

The paper is structured as follows: Section 2 deals with the modeling of the volumetric machining accuracy with consideration of the geometric error. The machining accuracy reliability analysis based on the Fast Markov chain simulation method is presented in Section 3. The sensitivity analysis based on the integration of the failure probability to identify the critical geometric errors is presented in Section 4. In Section 5, the results of the experimental validation are discussed. In this work, a vertical machining center was selected as an example to validate the proposed analysis method. The conclusions are presented in Section 6.

2. Volumetric error modeling by MBS theory

In this research, a 4-axis CNC machine tool, whose wire frame structure model is shown in Fig.1, was chosen as an example to demonstrate the core concepts of the proposed methods, and its main technical parameters are listed in Table 1. For a 4-axis machine tool, there are 24 position-dependent geometric errors and 5 position-independent geometric errors when the machine tool is modeled as a set of rigid bodies according to MBS theory. The different geometric errors are listed in Table 2.

Table 1. Main technical parameters of the 4-axis CNC machine tool used as an example in this study.

Configuration of the machine tool modules		**Parameters**
Workbench	Dimensions	2-630 mm×630 mm
	Maximum weight of the workpiece	1200kg
	Minimum indexing angle of the workbench	0.001°
Working range	Range in X-direction	1000mm
	Range in Y-direction	900mm
	Range in Z-direction	900mm
	Range of motion for the rotation around the A-axis	360°

2.1. Topological structure and geometric errors

This 4-axis machine tool has four slides that can be moved relative to each other. The two other bodies that are fixed to the machine are the tool and the workpiece. Table 3 illustrates the degrees of freedom between each pair of bodies with respect to the constraints, where "0" means no degree of freedom and"1" means one degree of freedom.

Based on MBS theory, various parts of the machine can be de-

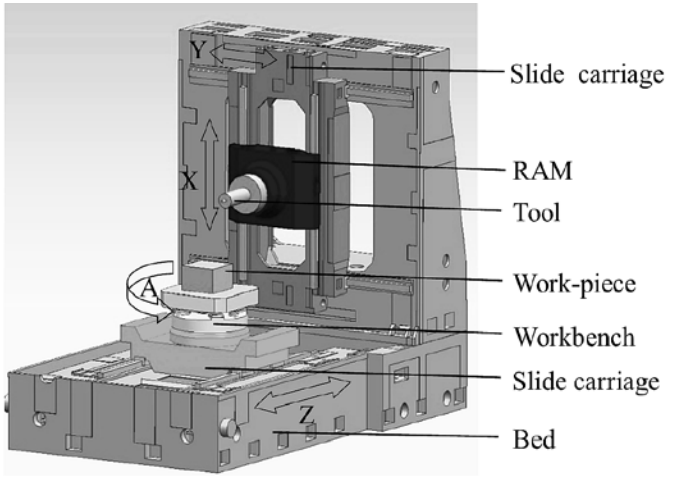

Fig. 1. Schematic illustration of the 4-axis horizontal precision machining center used as an example in this study.

Table 2. Geometric errors for the horizontal precision machining center

Axis	Error term	Sym-bol
X-axis	Positioning error	Δx_X
	Y-direction component of the straightness error	Δy_X
	X-direction component of the straightness error	Δz_X
	Rolling error	$\Delta \alpha_X$
	Britain swing error	$\Delta \beta_X$
	Yaw error	$\Delta \gamma_X$
Y-axis	*X*-direction component of the straightness error	Δx_Y
	Positioning error	Δy_Y
	Z-direction component of the straightness error	Δz_Y
	Rolling error	$\Delta \alpha_Y$
	Britain swing error	$\Delta \beta_Y$
	Yaw error	$\Delta \gamma_Y$
Z-axis	*X*-direction component of the straightness error	Δx_Y
	Y-direction component of the straightness error	Δy_Z
	Positioning error	Δz_Z
	Rolling error	$\Delta \alpha_Z$
	Britain swing error	$\Delta \beta_Z$
	Yaw error	$\Delta \gamma_Z$
A-axis	Run out error of the A-axis	Δx_A
	Run out error in Y-direction	Δy_A
	Run out error in Z-direction	Δz_A
	Angular error around A-axis	$\Delta \alpha_A$
	Angular error around Y-axis	$\Delta \beta_A$
	Angular error around Z-axis	$\Delta \gamma_A$
Orientation error	*X,Y*-axis perpendicularity error	$\Delta \gamma_{XY}$
	X,Z-axis perpendicularity error	$\Delta \beta_{XZ}$
	Y,Z-axis perpendicularity error	$\Delta \alpha_{YZ}$
	Parallelism of the X-axis and the A-axis in the Z-direction	$\Delta \beta_{ZA}$
	Parallelism of the X-axis and the A-axis in the Y-direction	$\Delta \gamma_{YA}$

Table 3. Degrees of freedom of the different two-body pairs of the precision horizontal machining center.

Adjacent bodies	Directions					
	X	Y	Z	α	β	γ
0-1	0	1	0	0	0	0
1-2	1	0	0	0	0	0
2-3	0	0	0	0	0	0
0-4	0	0	1	0	0	0
4-5	0	0	0	1	0	0
5-6	0	0	0	0	0	0

scribed just as an arbitrary classical body in terms of the geometric structure, and the machine tool can be treated as a MBS[17, 25].

As shown in Fig. 2, the 4-axis machine tool can be described as a structure with a double-stranded topology in which the first branch is composed of the bed, the slide carriage (Y-axis), the RAM (X-axis) and the tool. The second branch is composed of the bed, the slide carriage (Z-axis), the workbench (A-axis), and the workpiece. The bed is set as the inertial reference frame and denoted as body B_0, and the slide carriage (Y-axis) is denoted as body B_1. According to the natural growth sequence, the bodies are sequentially numbered along the direction away from the body B_1 from one branch to the other branch [11]. Fig. 2 illustrates the topology diagram for the machine tool. Table 4 shows the lower body array for the selected precision horizontal machining center.

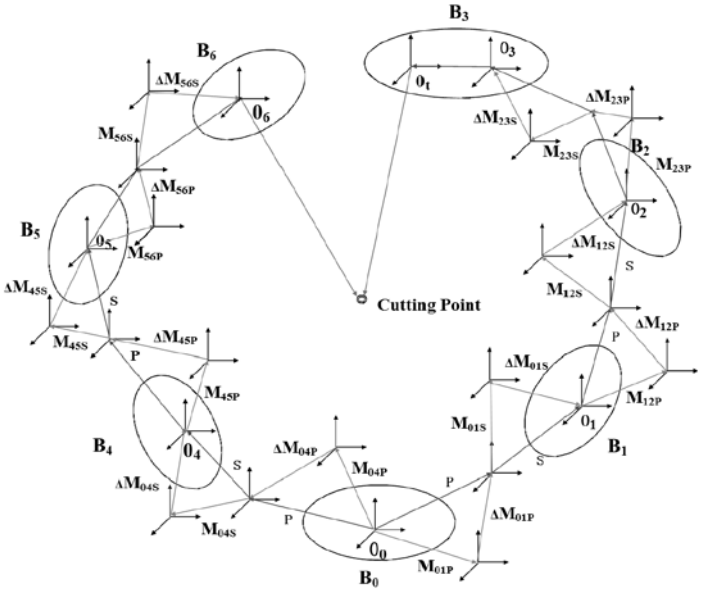

Fig. 2 Topological graph for the precision horizontal machining center. B_0-bed; B_1-slide carriage (Y-axis); B_2-RAM (X-axis); B_3-tool; B_4-Slide carriage (Z-axis); B_5-workbench (A-axis); B_6-workpiece

A rigid solid body has six degrees of freedom. These six coordinates uniquely specify the position of a rigid body in 3D space[2]. Each body B_i has 6 independent geometric errors Δx_h, Δy_h, Δz_h, $\Delta\alpha_h$, $\Delta\beta_h$ and $\Delta\gamma_h$. Δx_h, Δy_h and Δz_h are translational errors. $\Delta\alpha_h$, $\Delta\beta_h$ and $\Delta\gamma_h$ are rotational errors and are referred to as pitch, roll and yaw. The subscript h denotes the direction of motion, i.e., either X, Y, Z or A. There are five squareness errors, i.e., $\Delta\gamma_{XY}$, $\Delta\beta_{XZ}$, $\Delta\alpha_{YZ}$, $\Delta\gamma_{YA}$ and $\Delta\beta_{ZA}$ between the motion axis.

Table 4. Lower body array for the precision horizontal machining center.

Classical Body *j*	1	2	3	4	5	6
	1	2	3	4	5	6
	0	1	2	0	4	5
	0	0	1	0	0	4
	0	0	0	0	0	0

2.2. Generalized coordinates and characteristic matrixs

In order to normalize and make the machine tool accuracy modeling more convenient, special notations and conventions are needed for the coordinate system. The conventions used here are as follows: (1) Right-handed Cartesian coordinate systems were established for all the inertial components and the moving parts. These coordinates are generalized coordinates; the coordinate system on the inertial body is referred to as the reference coordinate system, and the coordinate systems on the other moving bodies are referred to as the moving co-

Table 5. Characteristic matrices for the precision horizontal machining center

Adjacent bodies	Body ideal static, motioncharacteristic matrix	Body static, kinematic error characteristic matrix
0-1	$\boldsymbol{M}_{01p}=\boldsymbol{I}_{4\times4}$ $\boldsymbol{M}_{01s}=\begin{bmatrix}1&0&0&0\\0&1&0&y\\0&0&1&0\\0&0&0&1\end{bmatrix}$	$\Delta\boldsymbol{M}_{01p}=\boldsymbol{I}_{4\times4}$ $\Delta\boldsymbol{M}_{01s}=\begin{bmatrix}1&-\Delta\gamma_Y&\Delta\beta_Y&\Delta x_Y\\\Delta\gamma_Y&1&-\Delta\alpha_Y&\Delta y_Y\\-\Delta\beta_Y&\Delta\alpha_Y&1&\Delta z_Y\\0&0&0&1\end{bmatrix}$
1-2	$\boldsymbol{M}_{12p}=\boldsymbol{I}_{4\times4}$ $\boldsymbol{M}_{12s}=\begin{bmatrix}1&0&0&x\\0&1&0&0\\0&0&1&0\\0&0&0&1\end{bmatrix}$	$\Delta\boldsymbol{M}_{12p}=\begin{bmatrix}1&-\Delta\gamma_{XY}&0&0\\\Delta\gamma_{XY}&1&0&0\\0&0&1&0\\0&0&0&1\end{bmatrix}$ $\Delta\boldsymbol{M}_{12s}=\begin{bmatrix}1&-\Delta\gamma_X&\Delta\beta_X&\Delta x_X\\\Delta\gamma_X&1&-\Delta\alpha_X&\Delta y_X\\-\Delta\beta_X&\Delta\alpha_X&1&\Delta z_X\\0&0&0&1\end{bmatrix}$
2-3	$\boldsymbol{M}_{23p}=\boldsymbol{I}_{4\times4}$ $\boldsymbol{M}_{23p}=\boldsymbol{I}_{4\times4}$	$\Delta\boldsymbol{M}_{23p}=\boldsymbol{I}_{4\times4}$ $\Delta\boldsymbol{M}_{23p}=\boldsymbol{I}_{4\times4}$
0-4	$\boldsymbol{M}_{04p}=\boldsymbol{I}_{4\times4}$ $\grave{\boldsymbol{I}}_{04s}=\begin{bmatrix}1&0&0&0\\0&1&0&0\\0&0&1&z\\0&0&0&1\end{bmatrix}$	$\Delta\boldsymbol{M}_{04p}=\begin{bmatrix}1&0&\Delta\beta_{XZ}&0\\0&1&-\Delta\alpha_{YZ}&0\\-\Delta\beta_{XZ}&\Delta\alpha_{YZ}&1&0\\0&0&0&1\end{bmatrix}$ $\Delta\boldsymbol{M}_{04s}=\begin{bmatrix}1&-\Delta\gamma_Z&\Delta\beta_Z&\Delta x_Z\\\Delta\gamma_Z&1&-\Delta\alpha_Z&\Delta y_Z\\-\Delta\beta_Z&\Delta\alpha_Z&1&\Delta z_Z\\0&0&0&1\end{bmatrix}$
4-5	$\boldsymbol{M}_{45p}=\boldsymbol{I}_{4\times4}$ $\grave{\boldsymbol{I}}_{45s}=\begin{bmatrix}1&0&0&0\\0&\cos A&-\sin A&0\\0&\sin A&\cos A&0\\0&0&0&1\end{bmatrix}$	$\Delta\boldsymbol{M}_{45p}=\begin{bmatrix}1&-\Delta\gamma_{YA}&\Delta\beta_{ZA}&0\\\Delta\gamma_{YA}&1&0&0\\-\Delta\beta_{ZA}&0&1&0\\0&0&0&1\end{bmatrix}$ $\Delta\boldsymbol{M}_{45s}=\begin{bmatrix}1&-\Delta\gamma_A&\Delta\beta_A&\Delta x_A\\\Delta\gamma_A&1&-\Delta\alpha_A&\Delta y_A\\-\Delta\beta_A&\Delta\alpha_A&1&\Delta z_A\\0&0&0&1\end{bmatrix}$
5-6	$\boldsymbol{M}_{56p}=\boldsymbol{I}_{4\times4}$ $\boldsymbol{M}_{56s}=\boldsymbol{I}_{4\times4}$	$\Delta\boldsymbol{M}_{56p}=\boldsymbol{I}_{4\times4}$ $\Delta\boldsymbol{M}_{56s}=\boldsymbol{I}_{4\times4}$

ordinate systems. (2) Each coordinate system's X-, Y-, Z-axis should be parallel to the X-, Y-, Z-axis of the other coordinate systems [23].

In MBS theory, the relation between the classical bodies of MBS can be expressed bymatrices. The characteristic matrices established for the selected machining center are listed in Table 5.

The coordinate of the tool forming point in the coordinate system of the tool is:

$$\boldsymbol{P}_t = \left[P_{tx}, P_{ty}, P_{tz}, 1 \right]^{\mathrm{T}} \tag{1}$$

and the coordinate of the workpiece forming point in the coordinate system of the workpiece can be written as:

$$\boldsymbol{P}_w = \left[P_{wx}, P_{wy}, P_{wz}, 1 \right]^{\mathrm{T}} \tag{2}$$

Ideally, the machine tool is without error; the tool forming point and the workpiece forming point will overlap together. As a result, the constraint equation for precision finishing under ideal conditions is given by:

$$\left[\prod_{k=n,L^n(t)=0}^{k=1} \boldsymbol{M}_{L^k(t)L^{k-1}(t)p} \boldsymbol{M}_{L^k(t)L^{k-1}(t)s} \right] \boldsymbol{P}_t = \left[\prod_{u=n,L^u(w)=0}^{u=1} \boldsymbol{M}_{L^u(w)L^{u-1}(w)p} \boldsymbol{M}_{L^u(w)L^{u-1}(w)s} \right] \boldsymbol{P}_{wideal} \tag{3}$$

By rearranging the terms, Eq. (3) can be rewritten as follows:

$$\boldsymbol{P}_{wideal} = \left[\prod_{u=n,L^u(w)=0}^{u=1} \boldsymbol{M}_{L^u(w)L^{u-1}(w)p} \boldsymbol{M}_{L^u(w)L^{u-1}(w)s} \right]^{-1} \left[\prod_{k=n,L^n(t)=0}^{k=1} \boldsymbol{M}_{L^k(t)L^{k-1}(t)p} \boldsymbol{M}_{L^k(t)L^{k-1}(t)s} \right] \boldsymbol{P}_t \tag{4}$$

The machining accuracy is finally related to the relative displacement error between the tool forming points of the machine and the workpiece. The constraint equation for precision finishing under actual conditions can be written as:

$$\boldsymbol{P}_{wactual} = \left[\prod_{u=n,L^n(w)=0}^{u=1} \boldsymbol{M}_{L^u(w)L^{u-1}(w)p} \Delta\boldsymbol{M}_{L^u(w)L^{u-1}(w)p} \boldsymbol{M}_{L^u(w)L^{u-1}(w)s} \Delta\boldsymbol{M}_{L^u(w)L^{u-1}(w)s} \right]^{-1} \times \left[\prod_{k=n,L^n(t)=0}^{k=1} \boldsymbol{M}_{L^k(t)L^{k-1}(t)p} \Delta\boldsymbol{M}_{L^k(t)L^{k-1}(t)p} \boldsymbol{M}_{L^k(t)L^{k-1}(t)s} \Delta\boldsymbol{M}_{L^k(t)L^{k-1}(t)s} \right] \boldsymbol{P}_t \tag{5}$$

The comprehensive volumetric error caused by the gap between the actual forming point and the ideal forming point can be expresses as:

$$\boldsymbol{E} = \left[\prod_{u=n,L^n(w)=0}^{u=1} \boldsymbol{M}_{L^u(w)L^{u-1}(w)p} \Delta\boldsymbol{M}_{L^u(w)L^{u-1}(w)p} \boldsymbol{M}_{L^u(w)L^{u-1}(w)s} \Delta\boldsymbol{M}_{L^u(w)L^{u-1}(w)s} \right] \boldsymbol{P}_{wideal} - \left[\prod_{k=n,L^n(t)=0}^{k=1} \boldsymbol{M}_{L^k(t)L^{k-1}(t)p} \Delta\boldsymbol{M}_{L^k(t)L^{k-1}(t)p} \boldsymbol{M}_{L^k(t)L^{k-1}(t)s} \Delta\boldsymbol{M}_{L^k(t)L^{k-1}(t)s} \right] \boldsymbol{P}_t \tag{6}$$

The comprehensive volumetric error mode of the horizontal precision machining center can be obtained from the characteristic matrices in Table 4 and Eq. (6). Similarly, the general volumetric error model for the machine tool can be established as follows:

$$\boldsymbol{E} = \boldsymbol{E}\left(\boldsymbol{G}, \boldsymbol{P}_t, \boldsymbol{P}\right) \tag{7}$$

where $\boldsymbol{E} = \left[E_X, E_Y, E_Z, 0\right]^{\mathrm{T}}$ is the volumetric error vector; $\boldsymbol{G} = [g_1, g_2, ..., g_{29}]^T$ is the vector consisting of 29 geometric errors, and $\Delta x_X, \Delta y_X, \Delta z_X, \Delta\alpha_X, \Delta\beta_X, \Delta\gamma_X, \Delta x_Y, \Delta y_Y, \Delta z_Y, \Delta\alpha_Y, \Delta\beta_Y, \Delta\gamma_Y, \Delta x_Z, \Delta y_Z, \Delta z_Z, \Delta\alpha_Z, \Delta\beta_Z, \Delta\gamma_Z, \Delta x_A, \Delta y_A, \Delta z_A, \Delta\alpha_A, \Delta\beta_A, \Delta\gamma_A, \Delta\gamma_{XY}, \Delta\beta_{XZ}, \Delta\alpha_{YZ}, \Delta\gamma_{YA}, \Delta\beta_{ZA} = g_1, g_2, g_3, g_4, g_5, g_6, g_7, g_8, g_9, g_{10}, g_{11}, g_{12}, g_{13}, g_{14}, g_{15}, g_{16}, g_{17}, g_{18}, g_{19}, g_{20}, g_{21}, g_{22}, g_{22}, g_{23}, g_{24}, g_{25}, g_{26}, g_{27}, g_{28}, g_{29}$; $\mathbf{P} = \left[x, y, z, 0\right]^{\mathrm{T}}$ represents the position vector of the motion axes of the machine center.

3. Machining accuracy reliability analysis based on Fast Markov Chain simulations

The machining accuracy reliability refers to the ability of the machine tool to perform at its specified machining accuracy under the stated conditions for a given period of time. In general, the volumetric machining errors can be decomposed into the corresponding X-, Y-, Z-direction components, and if the machining accuracy is lower than the specified requirement in the X-, Y- and Z-direction, respectively, the machining accuracy can be considered to be violated.

3.1. Failure mode and failure probability

The comprehensive volumetric error mode of the machine center can be written as:

$$\mathbf{E} = \mathbf{E}(\mathbf{G}) = \left[E_X(\mathbf{G}), E_Y(\mathbf{G}), E_Z(\mathbf{G}), 0 \right]^{\mathrm{T}} \tag{8}$$

The maximum permissible volumetric error of the machine tool is $\mathbf{e} = \left(e_X, e_Y, e_Z, 0\right)^{\mathrm{T}}$, where e_X, e_Y, e_Z indicates the maximum permissible volumetric error in X-, Y-, Z-direction, respectively, and the function matrix can be expressed as follow:

$$\mathbf{F} = \left[\mathbf{E} - \mathbf{e}\right] = \left[E_X(\mathbf{G}) - e_X, E_Y(\mathbf{G}) - e_Y, E_Z(\mathbf{G}) - e_Z, 0 \right]^{\mathrm{T}} == \begin{bmatrix} H_X(\mathbf{G}) \\ H_Y(\mathbf{G}) \\ H_Z(\mathbf{G}) \\ 0 \end{bmatrix} \tag{9}$$

The machining accuracy of the NC machine tool shows the following seven failure modes:

$$M_1 = \{H_X \geq 0,\ H_Y \leq 0 \text{ and } H_Z \leq 0\} \tag{10}$$

$$M_2 = \{H_X \leq 0,\ H_Y \geq 0 \text{ and } H_Z \leq 0\} \tag{11}$$

$$M_3 = \{H_X \leq 0,\ H_Y \leq 0 \text{ and } H_Z \geq 0\} \tag{12}$$

$$M_4 = \{H_X \geq 0,\ H_Y \geq 0 \text{ and } H_Z \leq 0\} \tag{13}$$

$$M_5 = \{H_X \geq 0,\ H_Y \leq 0 \text{ and } H_Z \geq 0\} \tag{14}$$

$$M_6 = \{H_X \leq 0,\ H_Y \geq 0 \text{ and } H_Z \geq 0\} \tag{15}$$

$$M_7 = \{H_X \geq 0, H_Y \geq 0 \text{ and } H_Z \geq 0\} \tag{16}$$

In Eqs.(10) to (12), M_1 M_2 and M_3 represent the cases where the machining accuracy of the machine tool in either the X-, Y- or Z-direction cannot meet the maximum permissible volumetric error. In Eqs.(13) to (15), M_4 M_5 and M_6 represent the cases where the machining accuracy of the machine tool cannot meet the maximum permissible volumetric error in two of the three directions. And In Eq.16, M_7 represent the case where the machining accuracy of the machine tool cannot meet the maximum permissible volumetric error in all of the three directions.

The failover domains for each of the failure modes are as follows:

$$F_1 = \left\{\mathbf{G}:\mathbf{G}\in H_X(\mathbf{G})\geq 0,\mathbf{G}\in H_Y(\mathbf{G})\leq 0 \text{ and } \mathbf{G}\in H_Z(\mathbf{G})\leq 0\right\} \quad (17)$$

$$F_2 = \left\{\mathbf{G}:\mathbf{G}\in H_X(\mathbf{G})\leq 0,\mathbf{G}\in H_Y(\mathbf{G})\geq 0 \text{ and } \mathbf{G}\in H_Z(\mathbf{G})\leq 0\right\} \quad (18)$$

$$F_3 = \left\{\mathbf{G}:\mathbf{G}\in H_X(\mathbf{G})\leq 0,\mathbf{G}\in H_Y(\mathbf{G})\leq 0 \text{ and } \mathbf{G}\in H_Z(\mathbf{G})\geq 0\right\} \quad (19)$$

$$F_4 = \left\{\mathbf{G}:\mathbf{G}\in H_X(\mathbf{G})\geq 0,\mathbf{G}\in H_Y(\mathbf{G})\geq 0 \text{ and } \mathbf{G}\in H_Z(\mathbf{G})\leq 0\right\} \quad (20)$$

$$F_5 = \left\{\mathbf{G}:\mathbf{G}\in H_X(\mathbf{G})\geq 0,\mathbf{G}\in H_Y(\mathbf{G})\leq 0 \text{ and } \mathbf{G}\in H_Z(\mathbf{G})\geq 0\right\} \quad (21)$$

$$F_6 = \left\{\mathbf{G}:\mathbf{G}\in H_X(\mathbf{G})\leq 0,\mathbf{G}\in H_Y(\mathbf{G})\geq 0 \text{ and } \mathbf{G}\in H_Z(\mathbf{G})\geq 0\right\} \quad (22)$$

$$F_7 = \left\{\mathbf{G}:\mathbf{G}\in H_X(\mathbf{G})\geq 0,\mathbf{G}\in H_Y(\mathbf{G})\geq 0 \text{ and } \mathbf{G}\in H_Z(\mathbf{G})\geq 0\right\} \quad (23)$$

In the reliability analysis of the machining accuracy, the failure probability P can be defined as the integral of the joint probability density function $f(\mathbf{G})$ for geometric errors in the failover domain F, so the failure probabilities of the different failure modes can be expressed as:

$$P_F^{(i)} = P\{\mathbf{G}\in F_i\} = \int\cdots\int_{F_i} f(\mathbf{G})\mathrm{d}\mathbf{G} \quad (24)$$

where, $i = 1,2\ldots7$, and i is the number of the failure modes.

The overall failure probability P_F of the machining accuracy can then be derived from basic principles of probability theory and statistics as follows:

$$P_F = P_F^{(1)} + P_F^{(2)} + P_F^{(3)} + P_F^{(4)} + P_F^{(5)} + P_F^{(6)} + P_F^{(7)} \quad (25)$$

3.2. Conversion of the correlated normal variables into independent standard normal variables

During actual processing, the geometric errors of the machine tool are correlated to each other and the effect of this correlation on the failure probability of the machining accuracy cannot be ignored. For a practical reliability analysis of the machining accuracy, in order to account for the actual situation, the correlation between the geometric errors of the machine tool must be taken into account. Therefore, the correlated geometric errors were first converted into independent standard normal random variables. Then, the reliability analysis method in independent space was used to determine the failure probability of the machining accuracy.

The n geometric errors of the machine tool can be represented as n-dimensional normal random variables $\mathbf{G} = (g_1, g_2, \ldots g_n)^{\mathrm{T}}$. Because the g eometric errors are correlated, the probability density function $f(\mathbf{G})$ of the geometric error vector $\mathbf{G}$ can be expressed as:

$$f(\mathbf{G}) = (2\pi)^{-\frac{n}{2}}|\mathbf{C_G}|^{-\frac{1}{2}}\exp\left[-\frac{1}{2}(\mathbf{G}-\boldsymbol{\mu}_\mathbf{G})^{\mathrm{T}}\mathbf{C_G}^{-1}(\mathbf{G}-\boldsymbol{\mu}_\mathbf{G})\right] \quad (26)$$

where:

$$\mathbf{C_G} = \begin{bmatrix} \sigma_{g_1}^2 & \rho_{g_1g_2}\sigma_{g_1}\sigma_{g_2} & \rho_{g_1g_3}\sigma_{g_1}\sigma_{g_3} & \cdots & \rho_{g_1g_n}\sigma_{g_1}\sigma_{g_n} \\ \rho_{g_1g_2}\sigma_{g_1}\sigma_{g_2} & \sigma_{g_2}^2 & \rho_{g_2g_3}\sigma_{g_2}\sigma_{g_3} & \cdots & \rho_{g_2g_n}\sigma_{g_2}\sigma_{g_n} \\ \rho_{g_1g_3}\sigma_{g_1}\sigma_{g_3} & \rho_{g_2g_3}\sigma_{g_2}\sigma_{g_3} & \sigma_{g_3}^2 & & \rho_{g_3g_n}\sigma_{g_2}\sigma_{g_n} \\ \vdots & \vdots & \vdots & & \vdots \\ \rho_{g_1g_n}\sigma_{g_1}\sigma_{g_n} & \rho_{g_2g_n}\sigma_{g_2}\sigma_{g_n} & \rho_{g_3g_n}\sigma_{g_2}\sigma_{g_n} & \cdots & \sigma_{g_n}^2 \end{bmatrix} \quad (27)$$

represents the covariance matrix of the geometric errors $\mathbf{G}$; $\mathbf{C_G}^{-1}$ is the inverse matrix of $\mathbf{C_G}$; $|\mathbf{C_G}|$ is the determinant of $\mathbf{C_G}$; and $\boldsymbol{\mu}_\mathbf{G} = (\mu_{g_1}, \mu_{g_2}, \ldots \mu_{g_n})^{\mathrm{T}}$ is the vector composed of the mean values of the geometric errors, μ_{g_i} and σ_{g_i} represent the mean value and the variance of geometric error $g_i\,(i = 1,2,3,\cdots,n)$, and $\rho_{g_ig_j}$ is the correlation coefficient of g_i and g_j.

According to the basic principles of linear algebra, there must be an orthogonal matrix $\mathbf{A}$ to convert the correlated normal variables $\mathbf{G} = (g_1, g_2, \cdots g_n)^{\mathrm{T}}$ into independent normal variables $\mathbf{y} = (y_1, y_2, \cdots y_n)^{\mathrm{T}}$ as follows:

$$f_Y(\mathbf{y}) = f_\mathbf{G}\left(\mathbf{A}^{-1}\mathbf{y} + \mu_\mathbf{G}\right) = (2\pi)^{-\frac{n}{2}}(\lambda_1\lambda_2\cdots\lambda_n)^{-\frac{1}{2}}\exp\left(-\frac{1}{2}\sum_{i=1}^{n}\frac{y_i^2}{\lambda_i}\right) \quad (28)$$

and:

$$\boldsymbol{y} = \mathbf{A}(\mathbf{G}-\boldsymbol{\mu}_\mathbf{G}), y_i \sim N(0,\lambda_i) \quad (29)$$

where, $\lambda_1, \lambda_2, \cdots \lambda_n$ are the eigenvalues of the covariance matrix $\mathbf{C_G}$. Furthermore, the column vectors of the orthogonal matrix $\mathbf{A}$ are equal to the orthogonal eigenvectors of the covariance matrix $\mathbf{C_G}$.

Based on the linear transformation $\boldsymbol{y} = \mathbf{A}(\mathbf{G}-\boldsymbol{\mu}_\mathbf{G})$, the correlated normal variables $\mathbf{G} = (g_1, g_2, \cdots g_n)^{\mathrm{T}}$ were converted to the independent normal variables $\mathbf{y} = (y_1, y_2, \cdots y_n)^{\mathrm{T}}$. Then, the independent normal variables $\mathbf{y} = (y_1, y_2, \cdots y_n)^{\mathrm{T}}$ were converted into independent standard normal random variables $\mathbf{u} = (u_1, u_2, \cdots u_n)^{\mathrm{T}}$ by using the following function.

$$u_i = \frac{\mathbf{y}_i - \boldsymbol{\mu}_{y_i}}{\sigma_{y_i}} = \frac{\mathbf{y}_i}{\sqrt{\lambda_i}}(i = 1,2,\cdots n) \quad (30)$$

Next, the failover domain $F(\mathbf{G})$ and the performance function $H(\mathbf{G})$ in the related space were converted to the failover domain $F(\mathbf{u})$. Finally, the failure probabilities of each failure modes can be rewritten as:

$$P_F^{(i)} = \int\cdots\int_{F_i(\mathbf{G})} f_G(\mathbf{G})d\mathbf{G} = \int\cdots\int_{F_i(\mathbf{y})} f_Y(\mathbf{y})d\mathbf{y} = \int\cdots\int_{F_i(\mathbf{u})} f_U(\mathbf{u})d(\mathbf{u}) \tag{31}$$

3.3. Fast Markov Chain simulation method for estimating the failure probability

There are many different methods to calculate the reliability of the machining accuracy based on numerical simulations which can be used for either analyzing the single failure mode-reliability or the multiple failure modes-reliability. However, the Markov chain method has so far not been used to analyze the reliability of the machining accuracy.

Because samples in the failover domain can be simulated efficiently by adopting the Markov chain method, for the general non-linear limit state equation $H_U(\mathbf{u})=H_G(\mathbf{G})=\begin{cases} H_X(\mathbf{G})=0 \\ H_Y(\mathbf{G})=0 \\ H_Z(\mathbf{G})=0 \end{cases}$, the Markov chain method can be used to determine the most probable failure point in the failover domain which is referred to as the design point. Through the design point, the linear limit state equation $L(\mathbf{u})=0$ which has the same design point has the non-linear limit state equation $H_U(\mathbf{u})=H_G(\mathbf{G})=\begin{cases} H_X(\mathbf{G})=0 \\ H_Y(\mathbf{G})=0 \\ H_Z(\mathbf{G})=0 \end{cases}$ can be obtained in the independent standard normal space.

Based on the multiplication theorem in probability theory, the following two equations can then be established.

$$P\{F_H \cap F_L\} = P\{F_H\}P\{F_L|F_H\} \tag{32}$$

$$P\{F_H \cap F_L\} = P\{F_L\}P\{F_H|F_L\} \tag{33}$$

where, $F_H=\{\mathbf{u}:\mathbf{u}\to\mathbf{G}\in F_i\}$, $F_L=\{\mathbf{u}:L(\mathbf{u})\le 0\}$, $P\{F_L\}=P\{L(\mathbf{u})\le 0\}$ and $P\{F_H\}=P\{F_i\}$. $P\{F_L|F_H\}$ and $P\{F_H|F_L\}$ are conditional probabilities.

Thus, the failure probability P_F can be expressed as follows:

$$P_F^{(i)} = P(F_i) = P\{F_H\} = P\{F_L\}\frac{P\{F_H|F_L\}}{P\{F_L|F_H\}} \tag{34}$$

where, $\dfrac{P\{F_H|F_L\}}{P\{F_L|F_H\}}$ can be defined as the scaling factor S:

$$S = \frac{P\{F_H|F_L\}}{P\{F_L|F_H\}} \tag{35}$$

Then Eq.(35) can be simplified as follows:

$$P_F^{(i)} = P\{F_L\}\bullet S \tag{36}$$

The probability density function of the samples which belong to the failover domain F_H can be expressed as follows:

$$q_H(\mathbf{u}|F_H) = \frac{I_H(\mathbf{u})f_U(\mathbf{u})}{P_H} \tag{37}$$

where, $I_H(\mathbf{u})$ is the indicator function of the non-linear performance function $H(\mathbf{u})$, and

$$I_H(\mathbf{u}) = \begin{cases} 1, & H(\mathbf{u})<0 \\ 0, & H(\mathbf{u})\ge 0 \end{cases} \tag{38}$$

According to the basic principles of Markov chain simulations, the transformation from one state to another state of the Markov chain is controlled by the proposal distribution function $f^*(\mathbf{å}|\mathbf{u})$. Both a symmetrical n-dimensional normal distribution and an n-dimensional uniform distribution can be used as a suggested distribution of the Markov chain. In this paper, the symmetrical n-dimensional uniform distribution was selected as the suggested distribution:

$$f^*(\mathbf{å}|\mathbf{u}) = \begin{cases} 1/\prod_{k=1}^{n} l_k, & |\varepsilon_k - u_k| \le \dfrac{l_k}{2} \\ 0, & \text{Others} \end{cases} \tag{39}$$

where, ε_k and u_k represent the k^{th} component of the n-dimensional vector $\mathbf{å}$ and $\mathbf{u}$ respectively. l_k represents the side length of the n-dimensional polyhedron in the u_k-direction, and $\mathbf{u}$ is the center of the n-dimensional polyhedron. Furthermore, l_k determines the maximum allowed distances from the next sample to the current sample.

Based on practical engineering experience and numerical algorithms, a point in the failover domain F_H was selected as the initial state of the Markov chain and denoted as u_0. The j^{th} state u_j of the Markov chain was then determined by the proposal distribution function and according to the Metropolis-Hastings guidelines based on the j-1th state u_{j-1}. First, a candidate state $\mathbf{å}$ was obtained through the proposal distribution function $f^*(\mathbf{å}|\mathbf{u}_{j-1})$. Then, the ratio r of the candidate state $\mathbf{å}$'s conditional probability density function and the state $\mathbf{u}_{j-1}$'s conditional probability density function can be expressed as follows:

$$r = q(\mathbf{å}|F_H)/\,q(\mathbf{u}_{j-1}|F_H) \tag{40}$$

At last, the next state $\mathbf{u}_j$ was determined according to the Metropolis-Hastings guidelines:

$$\mathbf{u}_j = \begin{cases} \text{å}, & \min\{1, r\} > \text{random}[0,1] \\ \mathbf{u}_{j-1}, & \min\{1, r\} \le \text{random}[0,1] \end{cases} \tag{41}$$

where, $\text{random}[0, 1]$ represents the random number which obeys the uniform distribution in $[0, 1]$.

N_H states $\{\mathbf{u}_0, \mathbf{u}_1, \cdots \mathbf{u}_{N_H-1}\}$ of the Markov chain can be generated via the above method, and they are sample points of the probability density function $q_H(\mathbf{u}|F_H)$. We selected the point which has the maximum value of $f_U(\mathbf{u})$ in the failover domain F_H from the N_H sample points of the probability density function $q_H(\mathbf{u}|F_H)$. This point is the maximum likelihood point and was denoted as $\mathbf{u}^* = (u_1^*, u_2^*, \cdots, u_n^*)$.

In the independent standard normal space, the linear limit state equation with the same maximum likelihood point of the failover domain F_H can be expressed as follows:

$$L(\mathbf{u}) = (\mathbf{0} - \mathbf{u}^*)(\mathbf{u} - \mathbf{u}^*)^{\mathrm{T}} = 0 \tag{42}$$

The corresponding probability of failure is:

$$P\{F_L\} = \Phi\left(-\sqrt{(u_1^*)^2 + (u_2^*)^2 + \cdots + (u_n^*)^2}\right) \tag{43}$$

where, $\Phi(\bullet)$ is the distribution function of the standard normal variable.

When plugging the N_H sample points into Eq.(42), the number of samples falling into $F_L = \{\mathbf{u} : L(\mathbf{u}) \le 0\}$ can be denoted as $N_{L|H}$.

Then, the estimation of the condition probability $P\{F_L | F_H\}$ can be written as follows:

$$\hat{P}\{F_L | F_H\} = \frac{N_{L|H}}{N_H} \tag{44}$$

Similarly, the condition probability $P\{F_H | F_L\}$ can be obtained using the Markov chain method to simulate the sample point in the failover domain F_L. The joint probability density function of the sample points in the failover domain F_L can be expressed as follows:

$$q_L(\mathbf{u}|F_L) = \frac{I_L(\mathbf{u}) f_U(\mathbf{u})}{P_L} \tag{45}$$

N_L sample points in the failover domain can be obtained through the Markov chain simulations. By plugging these sample points into $H(\mathbf{u})$ and calculating the values of $H(\mathbf{u})$, the number of sample points falling into the failover domain $F_H = \{\mathbf{u} : H(\mathbf{u}) \le 0\}$ can be obtained and recorded as $N_{H|L}$.

Then, the estimation of the condition probability $P\{F_L | F_H\}$ and the scaling factor S can be written as follows:

$$\hat{P}\{F_H | F_L\} = \frac{N_{H|L}}{N_L} \tag{46}$$

$$\hat{S} = \frac{\hat{P}\{F_H | F_L\}}{\hat{P}\{F_L | F_H\}} = \frac{N_{H|L}}{N_L} \bullet \frac{N_H}{N_{L|H}} \tag{47}$$

Because the machine tool has several failure modes, the failure probability of each failure mode should be calculated individually.

Let $F_H = F_i, i = 1, 2, \cdots 7$, then the $P\{F_L^{(i)}\}$ and $S^{(i)}$ corresponding to the failure modes can be obtained through.

$$P_F^{(i)} = P\{F_L^{(i)}\} S^{(i)} \quad i = 1, 2, \cdots 7 \tag{48}$$

The comprehensive failure probability of the machining accuracy can finally be expressed as follows:

$$\hat{P}_F = P_F^{(1)} + P_F^{(2)} + P_F^{(3)} + P_F^{(4)} + P_F^{(5)} + P_F^{(6)} + P_F^{(7)} \tag{49}$$

4. Machining accuracy reliability sensitivity analysis based on solving the integral of the failure probability

The machining accuracy reliability sensitivity coefficient is generally defined as the partial derivative of the failure probability for each failure mode with respect to the probability distribution parameters of the k^{th} geometric error. This can be expressed as follows:

$$S_{\mu_k}^{(i)} = \frac{\partial P_F^{(i)}}{\partial \mu_k} = \int \cdots \int_{F_i} \frac{\partial f(\mathbf{G})}{\partial \mu_k} \mathrm{d}\mathbf{G} \tag{50}$$

$$S_{\sigma_k}^{(i)} = \frac{\partial P_F^{(i)}}{\partial \sigma_k} = \int \cdots \int_{F_i} \frac{\partial f(\mathbf{G})}{\partial \sigma_k} \mathrm{d}\mathbf{G} \tag{51}$$

where, $i = 1, 2, \cdots, 7$; $k = 1, 2, \cdots, \mathrm{n}$; and n is the number of geometric errors. μ_k is the mean value of the k^{th} geometric error. σ_k is the standard deviation of k^{th} geometric errors. $S_{\mu_k}^{(i)}$ is the machining accuracy reliability sensitivity about the mean value μ_k with respect to the failure probability for i^{th} failure mode. $S_{\sigma_k}^{(i)}$ is the machining accuracy reliability sensitivity about the standard deviation σ_k with respect to the failure probability for the i^{th} failure mode.

Next, we defined the following regularized reliability sensitivity coefficients:

$$SA_{\mu_k}^{(i)} = \frac{\partial P_F^{(i)}}{\partial \mu_k} \frac{\sigma_k}{P_F^{(i)}} \tag{52}$$

$$SA_{\sigma_k}^{(i)} = \frac{\partial P_F^{(i)}}{\partial \sigma_k} \frac{\sigma_k}{P_F^{(i)}} \tag{53}$$

Then, we transformed Eqs.(52) and (53) into their corresponding integral form:

$$SA_{\mu_k}^{(i)} = \int \cdots \int_{F_i} \frac{\sigma_k}{f(\mathbf{G})} \frac{\partial f(\mathbf{G})}{\partial \mu_k} \left(\frac{f(\mathbf{G})}{P_F^{(i)}} \right) d\mathbf{G} \tag{54}$$

$$SA_{\sigma_k}^{(i)} = \int \cdots \int_{F_i} \frac{\sigma_k}{f(\mathbf{G})} \frac{\partial f(\mathbf{G})}{\partial \sigma_k} \left(\frac{f(\mathbf{G})}{P_F^{(i)}} \right) d\mathbf{G} \tag{55}$$

Obviously Eq. (54) and (55) can be expressed as the mathematical expectation in the failure domain F_i:

$$SA_{\mu_k}^{(i)} = E_{F_i}\left[\frac{\sigma_k}{f(\mathbf{G})} \frac{\partial f(\mathbf{G})}{\partial \mu_k} \right] \tag{56}$$

$$SA_{\sigma_k}^{(i)} = E_{F_i}\left[\frac{\sigma_k}{f(\mathbf{G})} \frac{\partial f(\mathbf{G})}{\partial \sigma_k} \right] \tag{57}$$

where, $E_{F_i}[\bullet]$ is the mathematical expectation in the failure domain F_i.

Through Eqs.(29) and (30), the sample points $\left\{\mathbf{u}_0^{(i)}, \mathbf{u}_1^{(i)}, \cdots \mathbf{u}_{N_H-1}^{(i)}\right\}$ can be converted to $\left\{\mathbf{G}_0^{(i)}, \mathbf{G}_1^{(i)}, \cdots \mathbf{G}_{N_H-1}^{(i)}\right\}$. By plugging $\left\{\mathbf{G}_0^{(i)}, \mathbf{G}_1^{(i)}, \cdots \mathbf{G}_{N_H-1}^{(i)}\right\}$ into the following formulas, the regularized reliability sensitivity coefficients can be eventually obtained:

$$\widehat{SA}_{\mu_k}^{(i)} = \frac{1}{N_H} \sum_{0}^{N_H-1} \frac{\sigma_k}{f(\mathbf{G})} \frac{\partial f(\mathbf{G})}{\partial \mu_k} \tag{58}$$

$$\widehat{SA}_{\sigma_k}^{(i)} = \frac{1}{N_H} \sum_{0}^{N_H-1} \frac{\sigma_k}{f(\mathbf{G})} \frac{\partial f(\mathbf{G})}{\partial \sigma_k} \tag{59}$$

Then, the general reliability sensitivity coefficients can be expressed as follows:

$$S_{\mu_k}^{(i)} = \frac{\partial P_F^{(i)}}{\partial \mu_k} = \widehat{SA}_{\mu_k}^{(i)} \bullet \frac{P_F^{(i)}}{\sigma_k} \tag{60}$$

$$S_{\sigma_k}^{(i)} = \frac{\partial P_F^{(i)}}{\partial \sigma_k} = \widehat{SA}_{\sigma_k}^{(i)} \bullet \frac{P_F^{(i)}}{\sigma_k} \tag{61}$$

5. Application and improvement

The machine tool shown in Fig.1 was selected as an example to demonstrate the method. The six position dependent geometric errors of each prismatic joint were directly measured using a dual-frequency laser interferometer[15] and an electronic level. XD sensor was used to receive and reflect the laser in the measurement process. And it was also used to detect the angle error and the straightness error of the measuring process. The squareness errors were measured using a dial indicator and a flat ruler. A photograph of the experimental setup is shown in Fig.3.

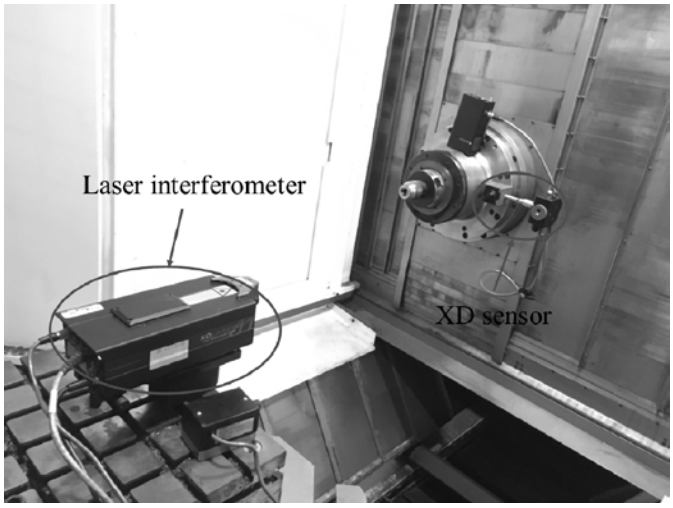

Fig.3 Photograph of the experimental setup.

Through a statistical analysis of the obtained sample data, the probability distribution of the geometric errors can be obtained. Taking the positioning error at Δx_x= 200mm, y=400mm, z=300mm as an example, the geometric error can be described by a normal distribution. Actually, the experimental results showed that each position-dependent geometric error can be described by a normal distribution [35]. Table 6 lists the values obtained for the position-independent errors. Table 7 compares the mean values (*M*) and the variance values (*V*) of the probability distributions used to describe the position-dependent geometric errors at x = 200mm, y = 400mm, z = 300mm.

Using the proposed method, the failure probabilities were calculated for each failure mode at *x*= 200 mm, y=400mm, z=300mm, and the results are listed in Table 8. The results of machining accuracy reliability sensitivity analysis are presented in Table 9.

Nine evenly spaced test points (a total of 33 test points) were selected along each body diagonal of the machine tool's working space, zas shown in Fig.4. The results of the sensitivity analysis at each test point were obtained using the method described above. Then, a sensitivity analysis for the whole working space was conducted employing the weighted average method.

The failure probability of failure mode M_i, at the test point "*j*", was defined as ${}^{j}P_F^{(i)}$, and the failure probability of failure mode M_i for the whole working space can be defined as $\widehat{P}_F^{(i)}$. Furthermore, the machining accuracy reliability sensitivity of the mean value μ_k of geometric error g_k for the i^{th} failure mode M_i, at the test point "*j*", was

Table 6. Values obtained for the position-independent errors.

Sequence Number	Parameter	Value(mm)
1		0.0039/500
2		0.0037/500
3		0.0037/500
4		0.012/300
5		0.012/300

Table 7. Probability distributions of position-dependent geometric errors

Sequence Number	Parameter	Probability distribution	M(mm)	V(mm^2)
1	Δx_x	normal distribution	0.0040	0.05/6
2	Δy_x	normal distribution	0.0039	0.05/6
3	Δz_x	normal distribution	0.0038	0.05/6
4	$\Delta \alpha_x$	normal distribution	0.0025/1000	0.03/6000
5	$\Delta \beta_x$	normal distribution	0.0027/1000	0.06/6000
6	$\Delta \gamma_x$	normal distribution	0.00242/1000	0.05/6000
7	Δx_y	normal distribution	0.0038	0.04/6
8	Δy_y	normal distribution	0.0040	0.05/6
9	Δz_y	normal distribution	0.0044	0.04/6
10	$\Delta \alpha_y$	normal distribution	0.00253/1000	0.05/6000
11	$\Delta \beta_y$	normal distribution	0.00242/1000	0.04/6000
12	$\Delta \gamma_y$	normal distribution	0.00224/1000	0.04/6000
13	Δx_z	normal distribution	0.0035	0.03/6
14	Δy_z	normal distribution	0.0041	0.03/6
15	Δz_z	normal distribution	0.0043	0.05/6
16	$\Delta \alpha_z$	normal distribution	0.00233/1000	0.03/6000
17	$\Delta \beta_z$	normal distribution	0.00259/1000	0.04/6000
18	$\Delta \gamma_z$	normal distribution	0.00252/1000	0.03/6000
19	Δx_A	normal distribution	0.0058	0.017/6
20	Δy_A	normal distribution	0.0062	0.021/6
21	Δz_A	normal distribution	0.0065	0.024/6
22	$\Delta \alpha_A$	normal distribution	0.00583/1000	0.02/6000
23	$\Delta \beta_A$	normal distribution	0.03219/1000	0.02/6000
24	$\Delta \gamma_A$	normal distribution	0.00692/1000	0.04/6000

Table 8. Failure probabilities of the different failure modes at x= 200 mm, y=400mm, z=300mm

Failure mode	M_1	M_2	M_3	M_4	M_5	M_6	M_7
Failure probability (%)	0.09	0.81	0.55	0.111	0.77	0.29	0.35

defined as ${}^{j}S_{\mu_k}^{(i)}$, and the machining accuracy reliability sensitivity of the variance σ_k of geometric error g_k at the test point "j", was defined as ${}^{j}S_{\sigma_k}^{(i)}$. Then, for the whole working space, the machining accuracy reliability sensitivity of the mean value μ_k and the variance σ_k of geometric error g_k for the i^{th} failure mode M_i, can be defined as $\hat{S}_{\mu_k}^{(i)}$ and $\hat{S}_{\sigma_k}^{(i)}$, respectively.

Table 9. Results of the machining accuracy reliability sensitivity analysis at x = 200mm, y = 400mm, z = 300mm

Geometric errors	Sensitivity coefficient						
	M_1	M_2	M_3	M_4	M_5	M_6	M_7
Δx_x	0.0304	0.0154	0.0681	0.0318	0.0493	0.0251	0.0789
Δy_x	0.0352	0.0858	0.0591	0.0432	0.0434	0.0842	0.0321
Δz_x	0.0010	0.0540	0.0135	0.0503	0.0430	0.0098	0.0278
$\Delta \alpha_x$	0.0572	0.0618	0.0697	0.0252	0.0334	0.0093	0.0205
$\Delta \beta_x$	0.0571	0.0390	0.0485	0.0005	0.0275	0.0742	0.0556
$\Delta \gamma_x$	0.0120	0.0516	0.0682	0.0817	0.0725	0.0539	0.0775
Δx_y	0.0122	0.0591	0.0348	0.0720	0.0364	0.0303	0.0458
Δy_y	0.0674	0.0405	0.0453	0.0369	0.0015	0.0270	0.0756
Δz_y	0.0488	0.0271	0.0632	0.0573	0.0419	0.0768	0.0396
$\Delta \alpha_y$	0.0341	0.0109	0.0649	0.0009	0.0058	0.0863	0.0458
$\Delta \beta_y$	0.0518	0.0369	0.0626	0.0117	0.0249	0.0176	0.0004
$\Delta \gamma_y$	0.011h8	0.0295	0.0085	0.0276	0.0387	0.0161	0.0170
Δx_z	0.0824	0.0133	0.0342	0.0860	0.0699	0.0638	0.0021
Δy_z	0.0798	0.0454	0.0155	0.0066	0.0677	0.0501	0.0689
Δz_z	0.0447	0.0406	0.0061	0.0586	0.0745	0.0871	0.0476
$\Delta \alpha_z$	0.0504	0.0496	0.0384	0.0443	0.0795	0.0078	0.0793
$\Delta \beta_z$	0.0205	0.0367	0.0659	0.0389	0.0091	0.0014	0.0398
$\Delta \gamma_z$	0.0864	0.0026	0.0361	0.0685	0.0613	0.0322	0.0433
Δx_A	0.0577	0.0382	0.0707	0.0741	0.0098	0.0552	0.0582
Δy_A	0.0271	0.0197	0.0064	0.0399	0.0494	0.0086	0.0302
Δz_A	0.0152	0.0581	0.0547	0.0362	0.0241	0.0224	0.0131
$\Delta \alpha_A$	0.0329	0.0496	0.0095	0.0415	0.0559	0.0597	0.0750
$\Delta \beta_A$	0.0017	0.0771	0.0434	0.0577	0.0097	0.0829	0.0046
$\Delta \gamma_A$	0.0821	0.0572	0.0128	0.0086	0.0707	0.0182	0.0213

$$\hat{S}_{\mu_k}^{(i)} = \frac{1}{33}\sum_{j=1}^{33} {}^{j}S_{\mu_k}^{(i)} \tag{62}$$

$$\hat{S}_{\sigma_k}^{(i)} = \frac{1}{33}\sum_{j=1}^{33} {}^{j}S_{\sigma_k}^{(i)} \tag{63}$$

The results obtained for the failure probabilities of the different failure modes and the machining accuracy reliability sensitivities of

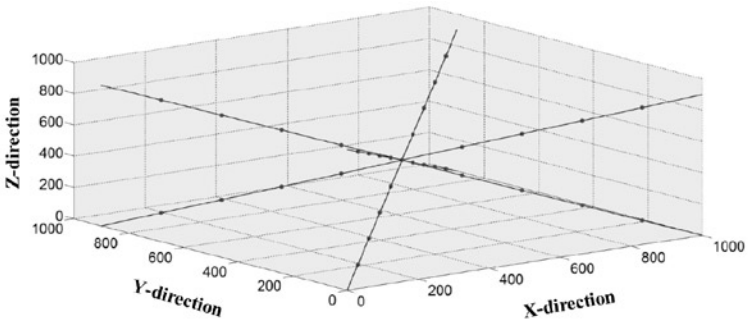

Fig. 4. Distribution of the test points.

Table 10. Failure probabilities of the different failure modes for the whole working space

Failure mode	M_1	M_2	M_3	M_4	M_5	M_6	M_7
Failure probability(%)	0.06	0.71	1.06	0.46	0.43	0.95	0.40

Table 11. Results of the machining accuracy reliability sensitivity analysis for the whole working space

Geometric errors	Sensitivity coefficient						
	M_1	M_2	M_3	M_4	M_5	M_6	M_7
Δx_x	0.0774	0.0358	0.0099	0.0318	0.0637	0.0305	0.0046
Δy_x	0.0082	0.0613	0.0089	0.0560	0.0160	0.0196	0.0296
Δz_x	0.0398	0.0236	0.0623	0.0577	0.0366	0.0691	0.0587
$\Delta \alpha_x$	0.0817	0.0032	0.0349	0.0442	0.0343	0.0164	0.0423
$\Delta \beta_x$	0.0134	0.0342	0.0173	0.0069	0.0572	0.0402	0.0441
$\Delta \gamma_x$	0.0381	0.0435	0.0083	0.0813	0.0226	0.0302	0.0883
Δx_y	0.0435	0.0083	0.0418	0.0306	0.0535	0.0412	0.0506
Δy_y	0.0247	0.0502	0.0119	0.0056	0.0713	0.0574	0.0436
Δz_y	0.0380	0.0364	0.0543	0.0509	0.0702	0.0226	0.0472
$\Delta \alpha_y$	0.0083	0.0483	0.0604	0.0249	0.0007	0.0174	0.0838
$\Delta \beta_y$	0.0623	0.0684	0.0413	0.0554	0.0429	0.0247	0.0059
$\Delta \gamma_y$	0.0539	0.0413	0.0414	0.0456	0.0599	0.0207	0.0822
Δx_z	0.0743	0.0690	0.0702	0.0362	0.0659	0.0071	0.0226
Δy_z	0.0289	0.0204	0.0737	0.0264	0.0273	0.0693	0.0147
Δz_z	0.0074	0.0237	0.0462	0.0603	0.0693	0.0555	0.0677
$\Delta \alpha_z$	0.0186	0.0167	0.0570	0.0175	0.0393	0.0416	0.0156
$\Delta \beta_z$	0.0296	0.0193	0.0318	0.0462	0.0190	0.0403	0.0624
$\Delta \gamma_z$	0.0724	0.0284	0.0785	0.0499	0.0676	0.0616	0.0835
Δx_A	0.0761	0.0261	0.0073	0.0606	0.0014	0.0682	0.0008
Δy_A	0.0411	0.0395	0.0448	0.0297	0.0114	0.0439	0.0457
Δz_A	0.0176	0.0687	0.0319	0.0821	0.0779	0.0284	0.0102
$\Delta \alpha_A$	0.0679	0.0871	0.0788	0.0651	0.0187	0.0680	0.0296
$\Delta \beta_A$	0.0350	0.0679	0.0549	0.0228	0.0087	0.0626	0.0396
$\Delta \gamma_A$	0.0419	0.0786	0.0322	0.0122	0.0646	0.0637	0.0267

the whole working space are listed in Table 10 and Table 11, respectively.

In order to study the machining accuracy reliability of the selected machining center in a real processing environment, the machining center has been used to machine a specific part. A photograph of the machining site is shown in Fig.5. The main parameters for the machining process are listed in Table 12.

In a modern advanced machining line, in order to improve the efficiency and production rhythm of the whole automatic production line, one machine only needs to complete one or just a few machining steps. For the selected machine, in a production line, it only needs to machine the machining surface of the reduction gearbox which has been marked in Fig.5. The machining quality of the machining surface is affected by the machining accuracy reliability of the machine center in the Z-direction. As shown in Eqs.(10) to (16), only M_3 , M_5 , M_6 and M_7 are related to the machining accuracy reliability of the machine center in Z-direction. As shown in Table 9, the failure probabilities of M_3 and M_6 are greater than the failure probabilities of M_5 and M_7 . So M_3 and M_6 are the critical failure modes which significantly affect the machining quality of the machining surface.

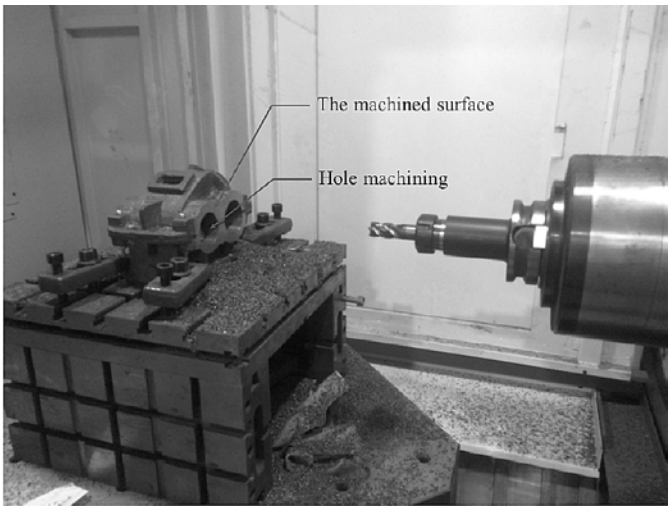

Fig.5 Photograph of the machining site.

As shown in Table 8, for failure mode M_3 , the sensitivity coefficients obtained for and were highest. For the failure mode M_6 , the sensitivity coefficient of and were the highest. Thus,, , and can be identified as the most crucial errors that affect M_3 and M_6 .

Because the geometric errors of the machine tool are linked to the geometric accuracy of the feeding components, there exist mapping relationships between the basic geometric errors and the accuracy parameters of the feeding components. The corresponding relationships between the basic geometric errors and the accuracy parameters of the components [2] are illustrated in Table 13.

Consequentially, the following modifications can be adopted to improve the machining accuracy: (1) Improving the straightness in the vertical plane of the X-guideway; (2) Improving the straightness in the horizontal plane of the Z-guideway; (3) Improving the parallelism of the Z-guideway; (4) Switching to a higher precision screw for the A-axis.

The failure probabilities of the different failure modes for the whole working space after modification were analyzed and are listed in Table 14. The comparison revealed that the failure probabilities were reduced after modification, and the failure probabilities of the failure modes and were greatly reduced after modification. Thus, we can conclude that the proposed machining accuracy reliability sensitivity analysis method is both feasible and effective.

Table 12. Main parameters of the machining process.

No	Tool	Illustration	Axial cutting depth (mm)	Radial cutting depth (mm)	Spindle speed (r/min)	Feed speed (mm/min)
1	Milling cutter F4AS2000ADL38	Rough machining	2	10	12000	4000
2	Boring tool SS20FBHS24	Precision boring machining	2	0.2	12000	2000
3	Face milling cutter D125	Finish-milling top surface	0.2	10	3000	3000

Table 13. Corresponding relationships between the basic geometric errors and the accuracy parameters of the components

Basic geometric errors	Accuracy parameters of the components
Δx_x, Δy_y and Δz_z	Cumulative pitch error of the lead screw
Δz_x, Δz_y and Δx_z	Straightness error in the vertical plane of the guideway
Δy_x, Δx_y and Δy_z	Straightness error in the horizontal plane of the guideway
$\Delta \alpha_x$, $\Delta \beta_y$ and $\Delta \gamma_z$	Parallelism error of the guideway
$\Delta \beta_x$, $\Delta \alpha_y$ and $\Delta \beta_z$	Straightness error in the vertical plane of the guideway and length of the moving parts
$\Delta \gamma_x$, $\Delta \gamma_y$ and $\Delta \alpha_z$	Straightness error in the horizontal plane of the guideway and length of the moving parts
Δx_A	Center distance deviation of the worm gear pairs
Δy_A	Center plane error of the worm gear pair
Δz_A	Radial pulsation of the turbine gear ring
$\Delta \alpha_A$	Cumulative pitch error of the gear pairs and length of the moving parts
$\Delta \beta_A$	Gear ring radial pulsation of the worm wheel and length of the moving parts
$\Delta \gamma_A$	Center distance deviation of the worm gear pairs and length of the moving parts

Table 14. Failure probabilities of the different failure mode for the whole working space after modification.

Failure mode	M_1	M_2	M_3	M_4	M_5	M_6	M_7
Failure probability (%)	0.058	0.70	0.60	0.46	0.40	0.61	0.36

6. Conclusions

In precision manufacturing, the geometric errors of a machine tool considerably affect the machining accuracy reliability of the machine tool, which directly determines the geometrical and dimensional accuracy of the machined product. Therefore, establishing the relationship between the geometric errors and the machining accuracy reliability and then efficiently improving the machining accuracy reliability are the key steps required to improve the achievable product quality.

In this paper, a new approach for analyzing the sensitivity of the machining accuracy reliability of machine tools based on fast Markov chain simulations was proposed. This method has the following two characteristics:

(1) The proposed analytical method can be used to establish the relationship between the model of the stochastic geometric errors and the machining accuracy reliability and to identify the key geometric errors that have the biggest impact on the machining accuracy reliability. According to the analysis results, the crucial geometric errors can be purposefully modified and the machining accuracy reliability can be dramatically improved. In addition, the results of the sensitivity analysis can also offer a good reference for an optimal design, accuracy control and error compensation of a complex machine.

(2) Employing the proposed analytical method, we identified seven failure modes of the machine tool. In a modern advanced machining line, in order to improve the efficiency and production rhythm of the whole automatic production line, one machine only needs to complete one or just a few machining steps. Considering the actual needs, the failure modes of the machine tools which need to be improved can be isolated, thereby greatly reducing the maintenance costs of machine tools.

Despite the progress, it should be pointed out that the geometric errors analyzed in this paper are quasi-static and correspond to cold-start conditions. The dynamic fluctuations caused by axis acceleration, dynamic load-induced errors and thermal errors were not taken into consideration. Therefore, the geometric errors under working conditions, which of course are of great practical significance, need to be further studied.

Acknowledgement

This work was financially supported by the National Natural Science Foundation of China (Grant No. 51575010, 51575009), the Beijing Nova Program (Grant No. Z1511000003150138), the Leading Talent Project of Guangdong Province, the Open Research Fund of the Key Laboratory of High Performance Complex Manufacturing, Central South University (Grant No. Kfkt2014-09), and the Shantou Light Industry Equipment Research Institute of Science and Technology Correspondent Station (Grant No. 2013B090900008).

References

1. Avontuur GC, van der Werff K. Systems reliability analysis of mechanical and hydraulic drive systems. Reliability Engineering & System Safety 2002; 77(2):121-130, http://dx.doi.org/10.1016/S0951-8320(02)00039-X.
2. Bohez EL, Ariyajunya B, Sinlapeecheewa C, et al. Systematic geometric rigid body error identification of 5-axis milling machines. Computer-aided design 2007b; 39(4): 229-244.
3. Cai L, Zhang Z, Cheng Q, Liu Z, Gu P. A geometric accuracy design method of multi-axis NC machine tool for improving machining accuracy reliability. Eksploatacja i Niezawodnosc – Maintenance and Reliability 2015; 17(1): 143-155, http://dx.doi.org/10.17531/ein.2015.1.19.
4. Çaydaş U, Ekici S. Support vector machines models for surface roughness prediction in CNC turning of AISI 304 austenitic stainless steel. Journal of Intelligent Manufacturing 2012; 23(3): 639-650, http://dx.doi.org/10.1007/s10845-010-0415-2.
5. Chen B, Chen X, Li B, et al. Reliability estimation for cutting tools based on logistic regression model using vibration signals. Mechanical Systems and Signal Processing 2011; 25(7): 2526-2537, http://dx.doi.org/10.1016/j.ymssp.2011.03.001.
6. Chen G, Liang Y, Sun Y, et al. Volumetric error modeling and sensitivity analysis for designing a five-axis ultra-precision machine tool. The International Journal of Advanced Manufacturing Technology 2013; 68(9-12): 2525-2534, http://dx.doi.org/10.1007/s00170-013-4874-4.
7. Cheng Q, Zhao H, Zhang G, et al. An analytical approach for crucial geometric errors identification of multi-axis machine tool based on global sensitivity analysis. The International Journal of Advanced Manufacturing Technology 2014, 75(1-4): 107-121, http://dx.doi.org/10.1007/s00170-014-6133-8.
8. De-Lataliade A, Blanco S, Clergent Y. Monte Carlo method and sensitivity estimations. Journal of Quantitative Spectroscopy and Radiative Transfer 2007; 75(5): 529-538, http://dx.doi.org/10.1016/S0022-4073(02)00027-4.
9. Du X, Sudjianto A, Huang B. Reliability-Based Design With the Mixture of Random and Interval Variables. Journal of Mechanical Design 2005; 127(6): 1068-1076, http://dx.doi.org/10.1115/1.1992510.

10. Eman KF, Wu BT, DeVries MF. A Generalized Geometric Error Model for Multi-Axis Machines. Annals of the CIRP 1987; 36(07): 253–256, http://dx.doi.org/10.1016/S0007-8506(07)62598-0.
11. Fu G, Fu J, Xu Y, et al. Product of exponential model for geometric error integration of multi-axis machine tools. The International Journal of Advanced Manufacturing Technology 2014; 71(9-12): 1653-1667, http://dx.doi.org/10.1007/s00170-013-5586-5.
12. Ghosh R, Chakraborty S, Bhattacharyya B. Stochastic Sensitivity Analysis of Structures Using First-order Perturbation. Meccanica 2001; 36(3): 291-296, http://dx.doi.org/10.1023/A:1013951114519.
13. Guo J, Du X. Reliability sensitivity analysis with random and interval variables. International Journal for Numerical Methods in Engineering 2009; 78(13): 1585-1617, http://dx.doi.org/10.1002/nme.2543.
14. Habibi M, Arezoo B, Nojedeh MV. Tool deflection and geometrical error compensation by tool path modification. International Journal of Machine Tools and Manufacture 2011; 51(6): 439-449, http://dx.doi.org/10.1016/j.ijmachtools.2011.01.009.
15. Homma T, Saltelli A. Importance measures in global sensitivity analysis of nonlinear models. Reliability Engineering & System Safety 1996; 52(1): 1-17, http://dx.doi.org/10.1016/0951-8320(96)00002-6.
16. Jha BK, Kumar A. Analysis of geometric errors associated with five-axis machining center in improving the quality of cam profile. International Journal of Machine Tools and Manufacture 2003; 43(6): 629-636, http://dx.doi.org/10.1016/S0890-6955(02)00268-7.
17. Kim K, Kim MK. Volumetric accuracy analysis based on generalized geometric error model in multi-axis machine tools. Mechanism and Machine Theory 1991; 26(2): 207-219, http://dx.doi.org/10.1016/0094-114X(91)90084-H.
18. Lei WT, Hsu YY. Accuracy enhancement of five-axis CNC machines through real-time error compensation. International Journal of Machine Tools and Manufacture 2003; 43(9): 871-877. http://dx.doi.org/10.1016/S0890-6955(03)00089-0.
19. Lin PD, Tzeng CS. Modeling and measurement of active parameters and workpiece home position of a multi-axis machine tool. International Journal of Machine Tools and Manufacture 2008; 48(3-4): 338-349, http://dx.doi.org/10.1016/j.ijmachtools.2007.10.004.
20. Liu H, Li B, Wang X, Tan G. Characteristics of and measurement methods for geometric errors in CNC machine tools. The International Journal of Advanced Manufacturing Technology 2011; 54(1-4): 195-201, http://dx.doi.org/10.1007/s00170-010-2924-8.
21. Liu YW. Applications of multi-body dynamics in the field of mechanical engineering. Chinese Journal of Mechanical Engineering 2000; 11(1): 144-149.
22. Lin TR. Reliability and failure of face-milling tools when cutting stainless steel. Journal of Materials Processing Technology 1998; 79(1): 41-46, http://dx.doi.org/10.1016/S0924-0136(97)00451-2.
23. Shin YC, Chin H, Brink MJ. Characterization of CNC machining centers. Journal of Manufacturing Systems 1991; 10(5): 407-421, http://dx.doi.org/10.1016/0278-6125(91)90058-A.
24. Stryczek R. A metaheuristic for fast machining error compensation. Journal of Intelligent Manufacturing 2014; 1-12, http://dx.doi.org/10.1007/s10845-014-0945-0.
25. Soons JA, Theuws FC, Schellekens PH. Modeling the errors of multi-axis machines: a general methodology. Precision Engineering 1992; 14(1): 5-19, http://dx.doi.org/10.1016/0141-6359(92)90137-L.
26. Tang J. Mechanical system reliability analysis using a combination of graph theory and Boolean function. Reliability Engineering & System Safety 2001; 72(1): 21-30, http://dx.doi.org/10.1016/S0951-8320(00)00099-5.
27. Tsutsumi M, Saito A. Identification of angular and positional deviations inherent to 5-axis machining centers with a tilting-rotary table by simultaneous four-axis control movements. International Journal of Machine Tools and Manufacture 2004; 44(12-13): 1333-1342, http://dx.doi.org/10.1016/j.ijmachtools.2004.04.013.
28. Xiao NC, Huang HZ, Wang Z, et al. Reliability sensitivity analysis for structural systems in interval probability form. Structural and Multidisciplinary Optimization 2011; 44(5): 691-705, http://dx.doi.org/10.1007/s00158-011-0652-9.
29. Xu C, Gertner G. Extending a global sensitivity analysis technique to models with correlated parameters. Computational Statistics & Data Analysis 2007; 51(12): 5579-5590, http://dx.doi.org/10.1016/j.csda.2007.04.003.
30. Yan S, Li B, Hong J. Bionic design and verification of high-precision machine tool structures. The International Journal of Advanced Manufacturing Technology 2015; 1-13, http://dx.doi.org/10.1007/s00170-015-7155-6.
31. Zhang Y M, Wen BC, Liu QL. Reliability sensitivity for rotor-stator systems with rubbing. Journal of Sound and Vibration 2003; 259(5): 1095-1107, http://dx.doi.org/10.1006/jsvi.2002.5117.
32. Zhu S, Ding G, Qin S, et al. Integrated geometric error modeling, identification and compensation of CNC machine tools. International Journal of Machine Tools and Manufacture 2012; 52(1): 24-29, http://dx.doi.org/10.1016/j.ijmachtools.2011.08.011.

Qiang CHENG
Bingwei SUN
Yongsheng ZHAO
Beijing Key Laboratory of Advanced Manufacturing Technology, Beijing University of Technology, Beijing 100124, China

Peihua GU
Department of Mechatronics Engineering, Shantou University, Shantou, Guangdong, 515063, China

Emails: chengqiang@bjut.edu.cn, 1359750743@qq.com, yszhao@bjut.edu.cn, gupeihua@aliyun.com